International Journal of Metallurgical &
Materials Science and Engineering (IJMMSE)
ISSN(P): 2278-2516; ISSN(E): 2278-2524
Vol. 5, Issue 1, Feb 2015, 39-52

EXPERIMENTAL ASPECTS OF DENSIFICATION AND ARC RADIUS OF BARRELLING CONSIDERING CIRCULAR ARC IN SINTERED P/M AISI 8640 STEEL DURING HOT UPSET POWDER PREFORM FORGING

Y. G. BALA[1], S. RAMANSANKARANARAYANAN[2] & K. S. PANDEY[3]

[1]Ph.D. Scholar, Department of Metallurgical and Materials Engineering, National Institute of Technology, Tiruchirappalli, Tamil Nadu, India

[2]Professor & Head, Department of Metallurgical and Materials Engineering, National Institute of Technology, Tiruchirappalli, Tamil Nadu, India

[3]Fromer Professor, Department of Metallurgical and Materials Engineering, National Institute of Technology, Tiruchirappalli, Tamil Nadu, India

ABSTRACT

Experimental work has been carried out to reveal quantitative data on some aspects of deformation and barrelling characteristics on hot deformation of sintered low alloy high strength AISI 8640 steel containing the composition of 0.4%C , 0.28%Si, 0.83%Mn, 0.5%Cr, 0.55%Ni and remaining 97.24%Fe, during axial hot upset forging at 1100°±10°C through powder preform forging in the way of powder metallurgy process. Cylindrical green compacts of three different aspect ratios of 0.6, 0.9and 1.2 were prepared from homogeneously blended powders respect to AISI 8640 steel composition in the pressure range of 480±10MPa with the compact density in the range of 85±1% of theoretical using 1.0MN capacity UTM. Sintering was carried out at 1100°±10°C for a period of 120 minutes in an electric muffle furnace under the protection of ceramic coating. Sintered compacts were hot upset forged to different height strains using 1.0MN capacity Friction Screw Press and quenched in the linseed oil bath to cool down to the room temperature. Analysis of experimental data and calculated parameters based on the forged preform geometry have resulted in several empirical relations relating Densification, Poisson's ratio, new Poisson's ratio and arc radius by considering circular arc of bulging.

KEYWORDS: Deformation, Densification, Sintering, Barrelling, Arc Radius, Circular Arc

INTRODUCTION

Powder Preform Forging (PPF) is the process in which sintered metal powder preforms are deformed in the partially open dies or in a confined dies or in the upsetting dies. The PPF is an extended powder metallurgy (P/M) method and valuable economic method of producing high strength and ductile parts from metal powders [1]. Further, hot forging is often employed in the initial stages of manufacturing of high quality steel parts where forging process offers an excellent demanding property like high yield strengths, high impact strengths with enhanced fatigue properties of the P/M products and also produces components essentially free from internal pores. The mass, density and the shape of the preforms are so closely controlled so as to ensure uniformity in the characteristics of the final forged components. The deformation process such as in forging methods lead to the plastic flow of sintered material in the direction perpendicular to the applied loads on the deforming preform/s. But, the frictional effects in the interfaces between the work piece and the loading surfaces lead to heterogeneous deformation inducing barrelling in the free surfaces [2]. The role of friction in bulk metal forming

has been carried out by many investigators and a comprehensive review of the literature has been published by Johnson and miller [3, 4]. However, in upset forging, the existence of the effects of frictional constraints existing between the sintered preform surfaces in contact with dies directly affect the plastic deformation which affects the preforms which undergoes heterogeneous deformation leading to barrelling of the preform[5]. Chen [6] developed a theoretical solution for the prediction of flow stresses during an upsetting operation considering the barrelling effects. Kulkarni and kalpakjain[7] found that bulging geometry is circular and that the initial ratio of height to diameter of the billet affects the bulging geometry. Schey et al. [8] presented a comprehensive report on the geometrical factors that affects the shape of the barrel. Narayanasamy and Pandey [9] carried out experimental work and theoretical analysis in sintered aluminium iron composite preforms under uniaxial stress state condition in order to evaluate the work hardening characteristics. Since during upsetting of porous P/M preforms there would be continuous reduction in the porosity contents and in turn, increased stresses would be required for further deformation resulting into the combined effects of densification as well as work hardening during cold working [10]. Powder forging process although possesses a wide potential for its adaptability in shaping various products, but the successful implementation of this process depends upon many complicated factors. However, the lack of understanding of these factors, has, in the past, given rise to unsuccessful performance of the products produced by this process. Though, this has resulted in early setbacks in adopting this process as an industrial venture, but, subsequently the process became foolproof. It is beyond any doubt that during forging of powder preforms, the densification as well as shape changes occur almost simultaneously in order to achieve full density and strong metallurgical bonds all across the collapsing pores inside the deforming P/M preforms, an additional work is required and hence additional strokes of press on the P/M preforms becomes mandatory. However, in initial low density P/M preforms, most of the work is spent initially on closing down the pores and again some additional work is required to attain optimum properties. Thus, the purpose of hot forging to get improved densification with the desired shape which is achieved by simultaneous application of temperature and pressure over unsintered and pre- sintered or sintered preforms made from metal powders. Therefore, the preform forging beautifully combines the advantages of conventional powder metallurgy such as dimensional accuracy and minimal material wastage coupled with high strengths of the forgings. Besides these significance in powder preform forging, the selected AISI8640 steel is a nickel -chrome - moly triple alloy steel is well known for toughness, wear resistance and the degree of hardness and also have been generally finds application in gears, crankshafts, screws, axles, pistons, and forged hand tools. The present experimental work has been undertaken to investigate the effects of initial perform geometry and composition on densification during hot upset forging of AISI 8640 sintered P/M steels. Barrelling in deforming preforms has been extensively investigated and its arc radius with increasing density has also been assessed. Circular barrelling has been investigated and new Poisson’s ratios as proposed by Narayanasamy and Pandey [9] have also been worked out while taking no account of barrelling and also taking account of barrelling. Thus, the present investigation highlights densification, Poisson’s ratio, bulging and evaluation of are radius for the system selected AISI8640 steels due to their industrial performance.

EXPERIMENTAL DETAILS

Materials Required

The materials required to conduct the present experimental investigation are, the elemental powder/s for the composition AISI8640 steel listed in “Table 1”, High Carbon High Chromium Die steel with suitable butt and punch set up and 1.0MN capacity UTM is required for the fabrication of green compacts. Graphite lubricant is required for lubricating the punch and die set up for consolidation and ejection of the green compacts. An electrical muffle furnace is required to

carry out sintering process. Friction Screw press of 1.0MN capacity is required to do the hot upset forging. Indigenously developed ceramic coating for the green compacts to protect them from the atmosphere against oxidation during sintering and forging preocess. The above mentioned powders are procured from the following companies: (a) Iron powder from TVS, Hyderabad, (b) elemental powders of Si, Mn, Mo, Cr and Ni were procured from Ghrishma Speciality Powders Limited , Mumbai, Maharastra and (c) Carbon in the form of Graphite from the Ashbury Graphite Mills Inc., Asbury Warrant Courtesy, New Jersey,USA.

Table 1: Per Centage Elementals Powders for AISI8640 Steel Composition

Elemental Powders	C	Si	Mn	Mo	Cr	Ni	Fe
% Composition	0.4	0.28	0.83	0.2	0.5	0.55	97.24

Powder Blend and Cold Compaction

Atomized iron powder of -180µm and other elemental powders listed in the "Table 1" of order -37µm are used for the preparation of the powder blend for the composition AISI8640 steel was weighed according the per centage weight and blended in the stainless steel pot mill along with ceramic ball with the weight ratio of powder to ball is 1:1 for a period of 36 hours so as to obtain homogeneous mixture. During the blending process the homogeneity of the powder is ensured for the properties like flow rate, apparent density, tap density by taking 100gm powder from the stainless steel pot mill for every one hour of blending using standard Hall- flow meter. The blending time and the homogeneity of the powder blends is stabilized when the consecutive readings for respective powder properties mentioned above being constant which are listed in "Table 2". The blended powder is compacted in the universal testing machine of 1.0MN capacity with aspect ratios 0.6, 0.9 and 1.2 respectively using the high carbon high chromium die setup. The compaction die, punch and butt were properly lubricated with graphite to avoid friction and poor surface finish during compaction. The powders were compacted with the pressure range of 480±10MPa.

Table 2: Powder Properties

Sl. No.	Property	AISI8640
1	Apparent Density, g/cc	3.415
2	Flow rate by Hall Flow meter Sec/50g	23.5
3	Tap density g/cc	4.42

Ceramic Coating ,Sintering and Upsetting

The green compacts are coated with indigenously developed ceramic coating to protect the compacts during sintering and forging against oxidation. This coating was done on the preform surface , two times perpendicular to each other and cured 12hrs in room temperature for each time of coating. The coated compacts after drying were kept in a tray and kept inside the electric muffle furnace. The temperature was raised up to $1100^{o}\pm10^{o}C$ in the muffle furnace and kept constant for a period of 120 minutes for the sintering time. The sintered compacts were hot upset forging to different height strains in the 1.0MN capacity friction screw press. And then these forged preforms were transferred to oil bath immediately after forging to cool down to the room temperature.

DIMENSIONAL MEASUREMENTS

The forged preforms were thoroughly cleaned and its height, contact diameter (top & bottom) and bulging diameter were measured. Minimum of five readings were taken and then averaged. Densities of the preforms are measured

using Archmedian's principle and keeping the density of water as 1g /cc. Using these measured parameters, respective analysis were made and discussed in result and discussions and also various conclusions has been drawn for these analysis.

THEORETICAL ANALYSIS

Once the porous P/M preform is subjected to axial compression, the axial strain induces lateral flow of material and flattening of press within the preform. Apart from this, the frictional constraints existing between the surfaces of the work piece and the tooling would result in barrelling. Figure 1 (a) , (b) and (c) shows the preform before and after deformation. Ideal deformation and the Barrelling or bulging encountered during upsetting considering circular arc are shown in Figure 1(b) and (c)

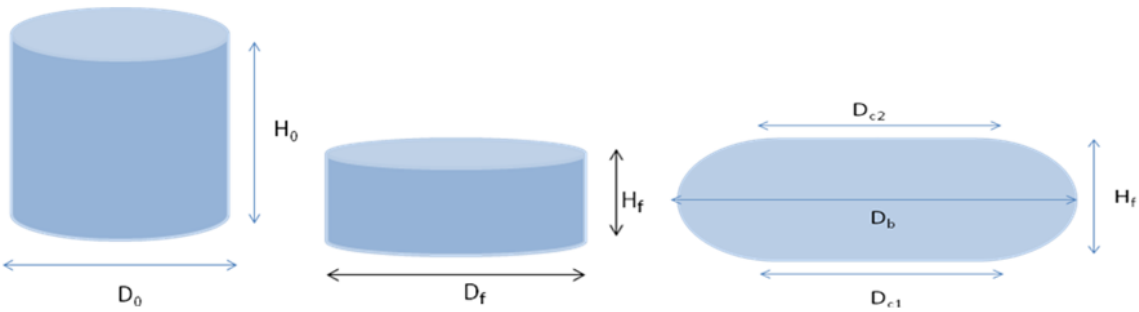

(a) Before Forging (b)After Forging (Ideal Condition) (c)After Forging (Considering Barrelling)

Figure 1: (a) ,(b),(c) Showing the Preform before Deformation (a) And After Deformation for Ideal Condition (b) And Circular Arc Barrelling(c)

Where **D_o –** initial preform density

H_o – initial preform height

ρ_o – initial preform density

D_{c1}- bottom contact diameter

D_{c2} – top contact diameter

D_c- average contact diameter

H_f – final preform height

D_b- bulged diameter

ρ_f – final density of the preform

Since the preform in consideration is porous in nature, therefore, volume constancy principle is not applicable. But, the mass constancy principle always remains valid ignoring the mass of pores if it contains air or any other gas. Now, therefore, applying mass constancy principle before and after deformation, the balance equation is as under, but considering no bulging, i.e., $D_b = D_c = D_{cf}$

$$\frac{\pi}{4} D_o^2 H_o \rho_o = \frac{\pi}{4} D_{cf}^2 H_f \rho_f \qquad (1)$$

$$\left(\frac{D_{cf}}{D_o}\right)^2\left(\frac{\rho_f}{\rho_o}\right) = \left(\frac{H_o}{H_f}\right)$$

$$\left(\frac{D_{cf}}{D_o}\right)^2\left(\frac{\rho_f}{\rho_{th}}\right) = \left(\frac{H_o}{H_f}\right)\left(\frac{\rho_o}{\rho_{th}}\right) \quad (2)$$

Where ρ_{th} is the theoretical density of the cent per cent dense mass. Now taking log on both sides of equation (2)

$$2\ln\left(\frac{D_{cf}}{D_o}\right) + \ln\left(\frac{\rho_f}{\rho_{th}}\right) = \ln\left(\frac{\rho_o}{\rho_{th}}\right) + \ln\left(\frac{H_o}{H_f}\right) \quad (3)$$

Further simplifying equations (3),

$$\frac{\ln\left(\frac{D_{cf}}{D_o}\right)}{\ln\left(\frac{H_o}{H_f}\right)} = \frac{\ln\left(\frac{\rho_o}{\rho_{th}}\right) - \ln\left(\frac{\rho_f}{\rho_{th}}\right)}{2} + \frac{1}{2}$$

Or

$$\frac{\ln\left(\frac{D_{cf}}{D_o}\right)}{\ln\left(\frac{H_o}{H_f}\right)} = \frac{1}{2} - \frac{1}{2}\ln\left(\frac{\rho_f}{\rho_o}\right)$$

But, $\frac{\ln\left(\frac{D_{cf}}{D_o}\right)}{\ln\left(\frac{H_o}{H_f}\right)} = \gamma_p$ = Poisson's ratio

Therefore, $\gamma_p = 0.5 - 0.5\ln\left(\frac{\rho_f}{\rho_o}\right)$ (4)

Derivation of Arc Radius for Circular Arc Barrelling

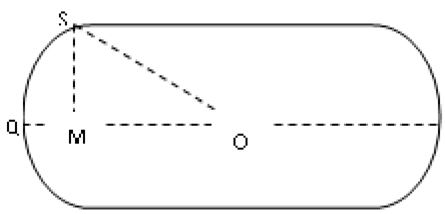

Figure 2: Dimensional Aspects Considering Circular Arc of Barrelling

From figure (2) OQ= R, MQ = X = $(D_b-D_c)/2$ and, OM = OQ-MQ= R-X

Now considering right angle triangle SMO and applying pythogorous theorem, the following equation is obtained:

$(OS)^2 = (OM)^2+(SM)^2$

$R^2 = (R-X)^2 + (H_f/2)^2$ (5)

$R^2= R^2-2RX+X^2+ (H_f^2/4)$

or $2RX - X^2 = H_f^2/4$ (6)

Since the value of x^2 is very small compared to R, the same can be ignored and thus equation (6) becomes

$2RX = H_f^2/4$

or $R = H_f^2/8X = H_f^2/4X\ (2X) = H_f^2/4(D_b-D_c)$

$$R = H_f^2/4(D_b-D_c) \tag{7}$$

Thus, the values of 'R' can be obtained at any strain value and can be plotted either against density or against strain.

New Poisson's ratio for Circular Arc Barrelling

During circular barrelling, the mass balance can be written as under:

$$\frac{\pi}{4}D_o^2H_o = \frac{\pi}{12}(2D_b^2 + D_c^2)\ \rho_f H_f \tag{8}$$

Or $D_o^2H_o\ (\rho_o/\rho_{th}) = \frac{1}{3}(2D_b^2+D_c^2H_f)\ (\rho_o/\rho_{th})$ (9)

Taking ln on both sides of equation (9)

$$\ln(\rho_o/\rho_{th}) - \ln(\rho_o/\rho_{th}) = \ln(H_o/H_f) - \ln[(2D_b^2+D_c^2)/(3D_o^2)]^2 \tag{10}$$

Here, $\varepsilon_H = \ln(H_o/H_f)$ and $\varepsilon_\Theta = \ln[(2D_b^2+D_c^2)/(3D_o^2)]$ (10a)

Equation (10) can be further simplified as:

$\ln\{(\rho_f/\rho_{th}) / \ln(\rho_o/\rho_{th})\} = \varepsilon_H - \varepsilon_\Theta$ (10b)

$\ln(\rho_f/\rho_o) = \varepsilon_H - \varepsilon_\Theta$

$(\rho_f/\rho_{th}) = (\rho_o/\rho_{th}) \exp^{\varepsilon H - \varepsilon \Theta}$

In this circular barrelling, the diameter strain as, $\ln[(2D_b^2+D_c^2)/(3D_o^2)]/2$ and height strain as $\ln(H_o/H_f)$, thus, the new Poisson's ratio γ_{pc} for circular arc, emerges as:

$$\gamma_{pc} = \ln[(2D_b^2+D_c^2)/(3D_o^2)]/2\ln(H_o/H_f) \tag{11}$$

RESULTS AND DISCUSSIONS

Densification and True Height Strains

"Figure 3" shows the curves drawn between the fractional theoretical density and the true height strains for three different aspect ratios of the AISI8640 steel composition during hot upset forging. Careful observation of these curves illustrates the influence of initial preform geometry all through the deformation and densification process. The curve corresponds to preform of lower aspect ratio is on top of the other two aspect ratio curves, which categorically shows that the lower aspect ratio preform is densified more as compared to the other two medium and largest aspect ratio preforms. This is due to the fact that the deformation during hot forging, the transformation of the load across the height direction is more rapid in lower aspect ratio preforms and least in the higher aspect ratio preforms. Further, the resistance offered during the significance of forging load experienced much in the larger aspect ratio preforms than the other two aspect ratio preforms.This is also due to the fact associated with the presence pores varying with different aspect ratios during the deformation process. The level of pore beds and pore closures in the lower aspect ratio preform is fewer and comparatively smooth which would have offered higher resistance during the deformation and densification. Hence, the larger aspect ratio preform densified poorly due to the preform experienced the higher damping and lower resistance during deformation on

hot upset forging. All these curves represent the similar characteristic nature for all the aspect ratio and they are found to conform to a third order polynomial of the form :

$$\rho_f/\rho_{th} = a_3\,(\varepsilon_h)^3 + a_2(\varepsilon_h)^2 + a_1(\varepsilon_h) + a_0 \quad (12)$$

Where, ρ_f/ρ_{th} is the fractional theoretical density, ε_h is true height strain, 'a_0','a_1', 'a_2' and 'a_3' are found to be empirically determined constants and they are shown in Table. The values of 'a_0' for all aspect ratios of this composition is very much close to initial preform density before hot forging , which almost equivalent to 0.85±0.01.The values of 'a_1' and 'a_3'were found to be positive and in the order of decending with respect to aspect ratios of 0.6, 0.9 and 1.2.

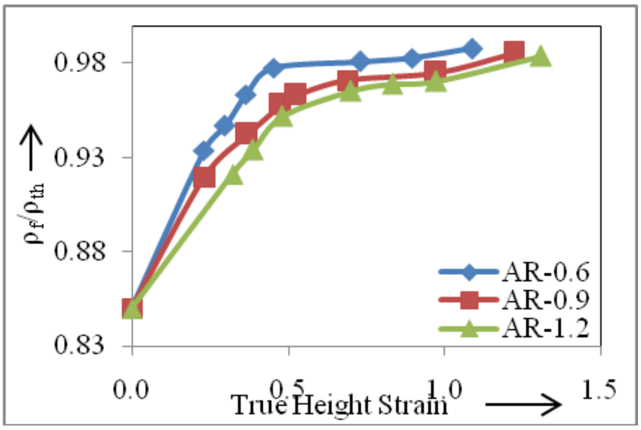

Figure 3: Relationship between Fractional Theoretical Density and True Height Strain for Different Aspect Ratio of AISI8640 Steel

Table 3: Coefficient Contants for Third Order Polynomial Mathematical Expression of the form $\rho_f/\rho_{th} = a_3\,(\varepsilon_h)^3 + a_2(\varepsilon_h)^2 + a_1(\varepsilon_h) + a_0$

Aspect Ratio	a_0	a_1	a_2	a_3	R^2
0.6	0.8492	0.5023	-0.6228	0.2554	0.9971
0.9	0.8496	0.3884	-0.4152	0.1538	0.9992
1.2	0.8491	0.3218	-0.2931	0.0960	0.9955

Therefore, this constant prop up the densification linearly as it are multiplied by the true height strain. In this period only a maximum densification is attained in the preforms.Further the 'a_2'values are found to be negative and has been always less than unity when the values are multiplied by the square of true height strain. Therefore, this constant will not have much effect on densification of the preforms.. Thus, this constant only smoothen the curves in the final stages of densification. Further,the 'R^2' value for each aspect ratio of the composition is extremely close to unity and hence the equation proposed is justified.

DEFORMATION, TRUE DIAMETER AND TRUE HEIGHT STRAINS

"Figures 4(a) and (b)" shows the plots drawn between the true diameter strains and the true height strains of sintered AISI8640 steel composition with respect to the three different aspect ratios consider the both friction and frictionless effect during the hot upset forging. "Figure 4(a)" represents the regular ideal deformation during the hot forging that means that there is no frictional constraint between the prefrom surfaces and the forging plates. Hence, there is no bulging at the periphery of the preforms as shown in "Figure 1(b)". "Figure 4(b)" shows the deformation considering the frictional constraint between the preform surfaces and the forging plates which leads to the bulging at periphery of the

preforms as in “Figure 1(c)”. Considering this subsequent bulging as circular arc and the curves plotted for each aspect ratios in the “Figures 4(a) and (b)” follows a similar characteristics nature and all data points lie below the theoretical line indicating the fact that the value of Poisson’s ratio will never be reached which mean that preforms would not densify completely under the upsetting mode. The curves corresponding to smallest aspect ratio preform is much nearer to the theoretical line and the curve corresponding to the largest aspect ratio preforms is at the farthest away from the theoretical line and the curves corresponding to medium sized aspect ratio remained in the middle of above curves. All these curves have been found to conform to a second order polynomial of the form:

$$\varepsilon_d = b_2(\varepsilon_h)^2 + b_1(\varepsilon_h) + b_0 \quad (13)$$

where, ε_d is the true diameter strain for ideal deformation , ε_{dc} is the diameter strain for circular arc barrelling , ε_h is the true height strain, ‘b_0’, ‘b_1’ and ‘b_2’are found to be empirically determined constant and they do depend upon initial geometry of the preforms.

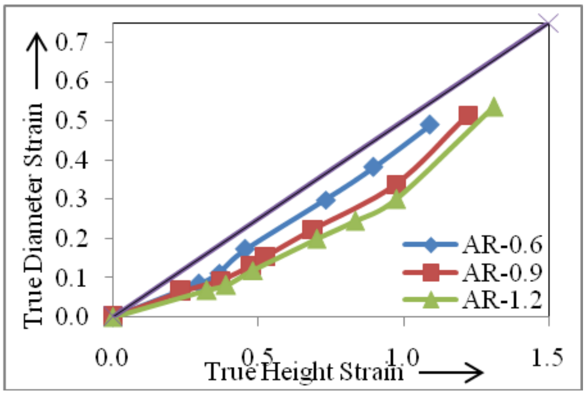

Figure 4(a): Relationship between True Diameter Strain and True Height Strain for Different Aspect Ratio of AISI8640 Steel for General

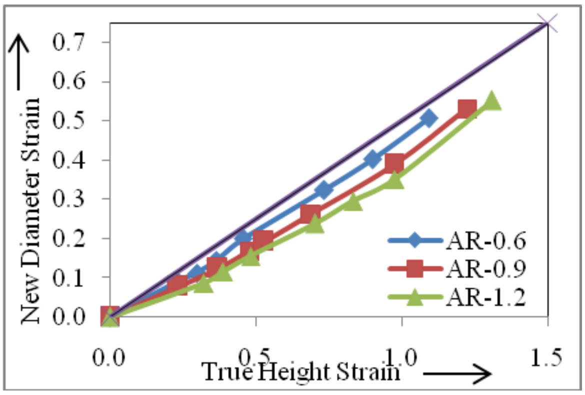

Figure 4(b): Relationship between True Diameter Strain and True Height Strain for Different Aspect Ratio of AISI8640 Steel for Circular Arc Bulging

Table 4: Coefficient Consants for Second Order Polynomial Mathematical Expression of the Form $\varepsilon_d = \varepsilon_{dc} = b_2(\varepsilon_h)^2 + b_1(\varepsilon_h) + b_0$

Bulging	Aspect Ratio	b_0	b_1	b_2	R^2
General	0.6	-0.0072	0.3031	0.1439	0.9973
	0.9	0.0054	0.1765	0.1902	0.9968
	1.2	0.0065	0.1094	0.2194	0.9961

Table 4: Contd.,

Circular Arc Bulging	0.6	-0.0025	0.3912	0.0687	0.9992
	0.9	0.0004	0.3023	0.1058	0.9996
	1.2	0.0012	0.2385	0.1366	0.9987

Examining all the constants listed in the "Table 4, it is found that the constant 'are in increasing order with respect to smaller aspect ratio to the largest aspect ratio preforms. The value of constant 'b_0'is very small and almost less than unity there is no effect on height strain or diameter strains. Further'b_1' and 'b_2' are positive and their contribute to the rise in the values of diameter strain as height strain is raised. Since, the regression coefficient 'R^2' values are found in the close proximity of unity and hence the above equation is valid for relating ε_d and ε_h for all aspect ratios considering both the friction as well as frictionless effect on hot upset mode of forging.

DENSIFICATION AND BULGING

"Figure 5" shows the plot drawn between the fractional theoretical density (ρ_f/ρ_{th}) and bulging ratio (D_b/D_0)for three different aspect ratios for the composition AISI8640 during hot upset forging. Observing these curves carefully, all the curves shows the similar characteristic nature and yielded a mathematical equation of third order polynomial of the form :

$$\rho_f/\rho_{th} = c_3(D_b/D_0)^3 - c_2(D_b/D_0)^2 + c_1(D_b/D_0) - c_0 \quad (14)$$

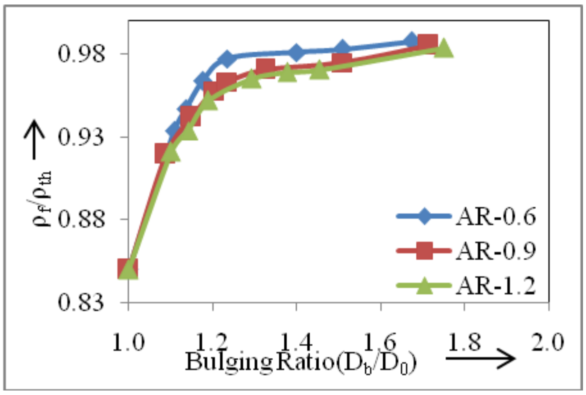

Figure 5: Relationship Between Fractional theoretical Density (ρ_f/ρ_{th}) and Bulging Ratio(D_b/D_0) for Different Aspect Ratio of AISI8640 Steel

Table 5: Coefficient Consants for Third Order Polynomial Mathematical Expression of the form : $\rho_f/\rho_{th} = c_3(D_b/D_0)^3 - c_2(D_b/D_0)^2 + c_1(D_b/D_0) - c_0$

Aspect Ratio	$-c_0$	c_1	$-c_2$	c_3	R^2
0.6	4.2174	10.876	7.5419	1.7341	0.9978
0.9	3.2941	8.8239	6.0572	1.3805	0.9948
1.2	3.1781	8.5552	5.8539	1.3282	0.9972

Where ρ_f/ρ_{th} is the fractional theoretical density , D_b/D_0 is the bulging ratio, 'c_0','c_1', 'c_2' and 'c_3' are the empirically determined constants which are tabulated in the "Table 5" . On observing the values of the constants from the "Table 5" , they are found to be in descending order with respect to smallest aspect ratio to largest aspect ratio preforms , which implies that the bulging is much more in smallest aspect ratio preforms when compared with other two aspect ratios preforms. This is reasonable that the smallest aspect ratio preforms achieved better densification during deformation process. However, the constants of 'c_1'and 'c_3' are being positive values, had facilitated the mechanism of densification

through out the hot upset forging .Whereas, 'c_0' and 'c_2' being negative, that had the only moderate or least effect on densification .The mathematical expression and the constants are also justified by the value of regression coefficient 'R^2'which is almost proximity to unity.

POISSON'S RATIO AND DENSIFICATION

"Figures 6(a) and (b)" represent the plots drawn between Poisson's ratio and the fractional theoretical density showing the influence of initial perform geometry considering the mode of deformation as general and circular bulging during hot upset forging. Observing these curves in each figure, it is found that the curve corresponding to the smallest aspect ratio preforms is much above than the curves corresponding to the largest and medium aspect ratio performs. Since all these curves are found to be characteristically similar in nature, they conform to a similar equation. However, the curve fitting has yielded a third order polynomial of the form :

$$\gamma_p = \gamma_{pc} = d_3(\rho_f/\rho_{th})^3 + d_2(\rho_f/\rho_{th})^2 + d_1(\rho_f/\rho_{th}) + d_0 \qquad (15)$$

Where 'γ_p' is the Poisson's ratio for ideal deformation, 'γ_{pc}' is the Poisson's ratio for circular arc bulging , ρ_f/ρ_{th} is the fractional theoretical density. 'd_0', 'd_1', 'd_3' and 'd_4' are the empirically determined constants and are tabulated in the "Table 6". These constants are also in the similar lessening order pattern with respect to the preforms of least to largest aspect ratios. The affirmative values in the "Table 6" uphold in boosting the densification , whereas, the negative values of the constants does not achieve any effect on densification, simply it flat terrain the densification with respect to the preform geometry. Further, it is found that the locality of the points of the curves consequent to cent per cent densification, the Poisson's ratio value attained had been 0.5 or less than 0.5 which is the case in the event of both an ideal as well as realistic deformation where barrelling is encountered.

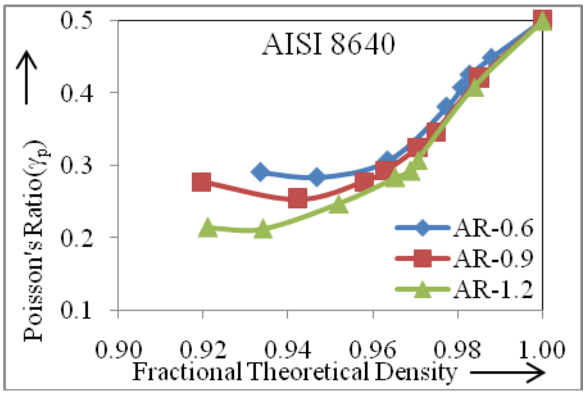

Figure 6(a): Relationship Between Poisson's Ratio(γ_p) and Fractional Theoretical Density (ρ_f/ρ_{th}) for Different Aspect Ratio of AISI8640 Steel for General

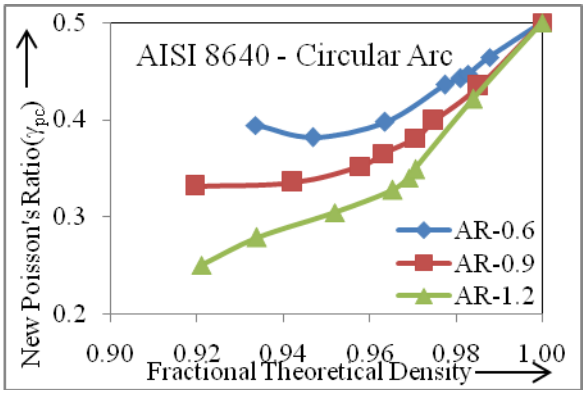

Figure 6 (b): Relationship Between Poisson's Ratio(γ_p) and Fractional Theoretical Density (ρ_f/ρ_{th}) for Different Aspect Ratio of AISI8640 Steel for Circular Arc Barrelling

Table 6: Coefficient Consants for Third Order Polynomial Mathematical Expression of the Form $\gamma_p = \gamma_{pc} = d_3(\rho_f/\rho_{th})^3 + d_2(\rho_f/\rho_{th})^2 + d_1(\rho_f/\rho_{th}) + d_0$

Bulging	Aspect Ratio	d_0	d_1	d_2	d_3	R^2
General	0.6	1359.2	-4167.7	4255.2	-1446.3	0.9906
	0.9	401.53	-1197.7	2285.6	-388.86	0.9949
	1.2	196.79	-564.34	532	-163.94	0.9918
Circular Arc	0.6	534.62	-1625.7	1646.1	-554.58	0.9986
	0.9	-26.683	115.43	-154.54	66.294	0.9989
	1.2	-447.34	1425.3	-1514.5	536.8	0.9916

DENSIFICATION AND BULGE RADIUS

"Figure 7" shows the plot drawn between radius of bulging and fractional theoretical density for three different aspect ratios considering the radius of bulging as the circular arc during hot upset forging. Each curve in this figure with respect to aspect ratios shows the similar characteristic nature which implies the influence of initial preform geometry on the bulge radius. The curve corresponding to the lowest aspect ratio it at the underneath. Whereas , the curve corresponding to the larger aspect ratio is on the top and the medium aspect ratio curve lies in the core of the other two curves. The characteristic nature of the arc radius drops down with increase in the fractional theoretical density , which implies that densification resulted in reduced arc of bulging for all aspect ratios. Further, all these curves conformed to a third order polynomial of the form :

$$R = f_3(\rho_f/\rho_{th})^3 + f_2(\rho_f/\rho_{th})^2 + f_1(\rho_f/\rho_{th}) + f_0 \quad (16)$$

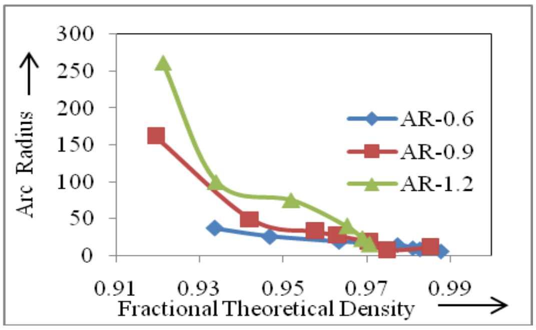

Figure 7 Relationship Between Arc Radius (R) and Fractional Theoretical Density(ρ_f/ρ_{th}) for Different Aspect Ratio of AISI8640 Steel for Circular Arc Barrelling

Table 7: Coefficient of the Constants for the Third Order Polynomial of the form : $R_a = f_3\,(\rho_f/\rho_{th})^3 + f_2(\rho_f/\rho_{th})^2 + f_1(\rho_f/\rho_{th}) + f_0$

Aspect Ratio	f_0	$-f_1$	fi_2	$-f_3$	R^2
0.6	294977	918972	954728	330744	0.9941
0.9	773273	2E+06	2E+06	844442	0.9906
1.2	7E+06	2E+07	2E+07	8E+06	0.9972

Where 'f_0','f_1', 'f_2' and 'f_3' are emperically determined constants and the values of the constants are tabulated in "Table 7". 'ρ_f/ρ_{th}' is the fractional theoretical density and 'R_a' is the arc radius for circular arc bulging Since the regression coefficient value 'R^2'is almost more than 0.99 the curve fitting is justified as the best fit.

CONCLUSIONS

Significant analysis of the experimental data and various calculated parameters and the different plots drawn for various relationships for the AISI 8640 steel developed through powder forging has give up the following main conclusions:

- All the relationship relating fractional theoretical density, height strain , diameter strain , poisson's ratio, new poisson's ratio bulging, arc radius has yielded a functional mathematical equation of either third order or second order polynomial with deterministic constant values . These polynomial equations are justified by its regression coefficient value R^2 almost proximity to the unity.
- With respect to the initial preform geometry , the smaller aspect ratio preforms densified effectively rather than other medium and higher aspect ratio preforms. This is due to the preforms experienced the rate of damping and resistance during deformation on hot upset forging.
- The plot drawn between the true diameter strain and true height strain for both ideal and circular arc bulging implies the effect of intial prefrom geometery on poisson's ratio. All the data points corresponding to the preforms are lie below the theoretical line indicating that the Poisson's ratio value attained had been 0.5 or less than 0.5 , even the preform attains the cent percent density.
- The arc radius of the bulging considering as the circular arc drops down with raise in the fractional theoretical density of all the preforms point outed that the influence of bulging and densification depends up on the initial preform geometry.

In general observation, it has been observed during experiment that mere to 40% to 50% height deformation, the crack on the free advancing surfaces tend to become more pronounced and therefore it is suggested that in actual practice of component production through forging route must involved the die constraints so as to block the flow of lateral movement and create a reweld the opening cracks and also create hydrostatic mode of loading which will makes the residual pores to be thermodynamically stable and hence the strength of the component will be retained. Over all, the present investigation has yielded various empirically relationship which can be employed for further applications.

REFERENCES

1. T.J.Griffith, R.Davis, M.B.Basset.(1977):*Compactability Equations for the Powder Forging Process*. Vol.4. (pp214 -220).Powder Metallurgy.

2. Hosford WF, Cadell RM .(1993). : *Metal Forming Mechanics and Metallurgy*. p 62 (Chapter 3) Prentice Hall, USA,
3. Johnson.W ,Mellor PB.(1975). : *Engineering Plasticity*. p 110-114(chapter 6).London Van Nostrand Reinhold.
4. Yang DY Choi Y, Kim JH.(2004). : *Analysis of Hot Upset Forging of Cylindrical Billets Considering the Dissimilar Frictional Conditions at Two Flat Die Surface*. p 44.vol 4. Int. Journal Mech. Tools Manufacturing
5. K.Manisekar, R.Narayanasamy. (2007). : *Effect of Friction on Barrelling in Square and Rectangular Billets of Aluminium during Cold Upset Forging*. vol.28. pp 592-598.Elsevier, Materials and Design.
6. Chen F.K. (2000). : *The Non Uniform Deformation of the Cylinder Compression Test*. pp 122-192. vol- 7. Journal of Engineering Material Technology – Trans ASME
7. Kulkarni KM, Kalpakjain S.A .(1969). : *Study on Barrelling as an Example of Free Deformation*. Vol -91, pp 743 -754. ASME Journal Eng., Ind.
8. Schey JA, Venner TR, Takomanask Sl. (1982). :*Shape Changes in the Upsetting of Slender Cylinders*. Vol – 104, pp 79-83.ASME Journal Eng., Ind.
9. Narayanasamy R, Pandey K.S.(1998). : *Some Aspects of Work Hardening in Sintered Aluminium - Iron Composite Preform during Cold Axial forming*. Vol- 84 136 -142. Journal of Material Process Technology.
10. Kahloe J. Void .(1971) . : *Behavior as influenced by pressure and plastic deformation*. p 10-6. Institute for metal forming report, Lehigh university Bethlehem PA. USA.